Available online at www.sciencedirect.com
ScienceDirect
Journal of Power Sources 162 (2006) 114–123
JOURNAL OF POWER SOURCES
www.elsevier.com/locate/jpowsour

DMFC employing a porous plate for an efficient operation at high methanol concentrations

Mohammad Ali Abdelkareem, Nobuyoshi Nakagawa *

Department of Biological and Chemical Engineering, Gunma University, 1-5-1 Tenjin, Kiryu, Gunma 375-8501, Japan

Received 18 May 2006; received in revised form 6 July 2006; accepted 7 July 2006
Available online 9 August 2006

Abstract

The effect of employing a porous carbon plate on the performance of a passive direct methanol fuel cell (DMFC) under closed circuit conditions was investigated. The porous carbon plate and a CO_2 gas layer that formed between the anode and the porous plate stably controlled the mass transfer of the methanol and water from the reservoir to the anode, which made operation with very high concentrations of methanol, even neat methanol, possible. The *i–V* and *i–t* performances of the DMFC with and without the porous plate were measured at different methanol concentrations, and the performances were compared. The maximum power density, 24 mW cm^{-2} at room temperature, obtained at 2 M without the porous plate was reproduced at 16 M with the porous plate. Also, the methanol crossover flux and water flux through the MEA was evaluated, and the Faraday efficiencies of the DMFC with and without the porous carbon plate were analyzed. When high concentrations of methanol were used with the porous plate, it was confirmed that the Faraday efficiency remained high, and the back diffusion of water from the cathode to the anode through the membrane occurred which resulted in no flooding at the cathode, contrary to the case without the porous plate. By increasing the distance between the anode and the porous plate, the power density decreased, suggesting that the distance of the CO_2 layer played an important role in obstructing the mass transport.

Keywords: Passive DMFC; Methanol crossover; Faraday efficiency; Neat methanol operation; Back diffusion; Porous plate

1. Introduction

There has been an increasing demand for the development of direct methanol fuel cells (DMFCs) [1–8] because of their high energy densities that are suitable for mobile electric devices and automobiles. However, the energy density of the DMFCs currently under development is still far from that expected due to the methanol crossover (MCO) and the high overvoltage at the electrodes [9–12]. Due to the methanol crossover, the DMFC usually shows the highest performance at low concentrations of methanol from 2 to 3 M [13,14] under active conditions and about 5 M [15–17] under passive conditions. To overcome the methanol crossover, a large number of studies [18–22] have been carried out for developing a new proton-conducting membrane with a low methanol permeability and high proton conductivity. Modification of the existing membranes like Nafion has also been conducted by making it a composite membrane [23–25] with inorganic or organic materials, surface modification by physical treatment [26] or by coating the surface with a thin film [27–29]. Only a few papers have considered the reducing ability of methanol crossover by mass transport control in the backing layer [30–32].

Another problem that decrease the DMFC power output, especially encountered in passive DMFCs with air breathing, is the flooding at the cathode [33,34]. The accumulation of water at the cathode causes a decrease and unstableness in the performance where the water blocks the openings of the porous cathode. The water at the cathode includes water produced by the oxygen reduction reaction, and that transported with protons from the anode as well as that generated by the oxidation of methanol that permeated through the membrane. The water has to be then smoothly removed from the cathode, or it should be controlled [35,36].

The authors demonstrated, in previous papers [30,31], that a passive DMFC with a porous plate as a support significantly reduced the methanol crossover and constantly regulated the cell

* Corresponding author. Tel.: +81 277 30 1458; fax: +81 277 30 1457.
E-mail address: nakagawa@bce.gunma-u.ac.jp (N. Nakagawa).

0378-7753/$ – see front matter © 2006 Elsevier B.V. All rights reserved.
doi:10.1016/j.jpowsour.2006.07.012

temperature. The mechanism of reducing the MCO was successfully explained by the diffusion control of the methanol through the porous plate. The transport and separation of methanol and water through the MEA with a porous plate under open circuit conditions were dependent on the properties of the porous material, i.e., thickness, porosity and water absorptivity of the porous material. It is expected that the DMFC employing the porous plate can be efficiently operated at high methanol concentrations and effectively achieve a high energy density for the DMFC systems.

In this study, it was investigated how the employment of a porous plate in a DMFC affects the performance under closed circuit conditions. A porous carbon plate was placed on the anode side and used to control the mass transfer from the methanol reservoir to the anode. The *i–V* and *i–t* performances at different methanol concentrations ranging from 1 to 24.7 M (neat methanol), were measured for the DMFC with and without the porous plate and their performances compared to each other. Also, in the *i–t* experiment, the methanol flux and water flux through the membrane electrode assembly (MEA) and Faraday efficiency were evaluated at different methanol concentrations. At the same time, the effect of the distance between the anode surface and porous plate on the performance was investigated. The mechanism of the cell performance with the porous plate was then discussed based on the mass transfer of the methanol and water at the anode.

2. Experimental

2.1. MEA preparation

The conventional MEA, which uses carbon cloth (35% Teflonized, ElectroChem, Inc.) as the anode and cathode backing layers, was prepared in the following manner. Pt black (HiSPEC 1000, Johnson Matthey Fuel Cells Co. Ltd.) and Pt–Ru black (HiSPEC 6000, Johnson Matthey Fuel Cells Co. Ltd.) were used as the catalyst for the cathode and anode, respectively. The catalyst ink was prepared by dispersing an appropriate amount of the catalyst in a solution of deionized water, isopropyl alcohol, and 5 wt.% Nafion solution (Wako, Inc.). The ink was then coated on the carbon cloth to make the electrodes. The catalyst loading was 10 mg cm^{-2} for each electrode, and the ionomer loading of the catalyst was 10 wt.% for the cathode and 15 wt.% for the anode. Nafion 112 was used as the electrolyte membrane. The MEA was then fabricated by sandwiching the membrane between the anode and the cathode and hot pressing them at 408 K and 5 MPa for 3 min.

2.2. Porous plate

A porous carbon plate, denoted as PCP hereafter, with a 2.0 mm thickness made of a composite of amorphous and graphite carbons, supplied from Mitsubishi Pencil Co. Ltd., was used in this study. The microstructure of the PCP measured using a mercury porosimeter, (Pascal 140 + 440, Thermo Finnigan, Inc.), revealed that it had a 0.543 cm^3 g^{-1} in total cumulative pore volume and 42.3 μm average pore diameter and 0.417 total porosity. The PCP was hydrophobic and its water absorptivity defined in our previous paper [31] was nearly zero.

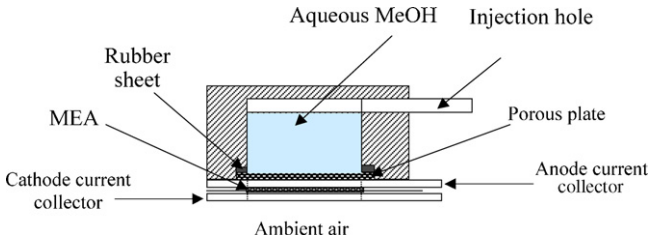

Fig. 1. Schematic diagram of the passive DMFC with or without the porous plate.

2.3. Passive DMFC with or without PCP

MEA with or without the porous plate was placed in a plastic holder as shown in Fig. 1. In the anode compartment, a methanol reservoir, 7 cm^3, was arranged. The MEA was sandwiched between two current collectors, which were stainless steel plates of 2 mm thickness with open holes for the passages of fuel and oxidant. The open ratio of the area for the active electrode was 73%. As a result of this configuration, methanol had to pass through the porous plate then through the openings of the anode current collector. Under closed circuit conditions, the openings of the anode current collector was filled with CO_2 gas which is enclosed between the porous plate and the anode. Therefore, a layer of CO_2 gas was formed between the porous plate and the anode, and the gas layer obstructs methanol transport from the reservoir to the anode. On the other hand, in the case of no PCP, CO_2 easily escaped through the opening of the anode current collector into the methanol solution as bubbles without preparing the CO_2 gas layer, and the solution is directly attached to the anode. Oxygen, from the surrounding air, diffused into the cathode catalyst layer through the openings of the cathode current collector.

2.4. Measurement of the cell performance

In this study, all the experiments were conducted in a complete passive mode at ambient conditions (293 K and 1 atm), methanol solutions with different concentrations were fed into the reservoir by a syringe through the injection hole, and left in the cell from a few minutes to 1 h based on the methanol concentration. We avoided direct contact of the MEA with the solution for a long time when the methanol concentration was high. The current–voltage, *i–V*, characteristics were measured by linear sweep voltammetry from the open circuit voltage to zero at the scan rate of 1 mV s^{-1}. After that, the current density versus time, *i–t* characteristic, at 0.1 V was measured for 5–12 h. These measurements were conducted using an electrochemical measurement system (HAG-5010, Hokuto Denko Co. Ltd.). The temperature of the cell was also measured using a thermocouple placed between the surface of the anode current collector and the porous plate.

At the end of the *i–t* experiments for a certain methanol concentration, the weight loss of the entire cell holder was measured

and the methanol concentration of the remaining solution in the reservoir was also measured by gas chromatography. Based on the results, methanol and water fluxes during the *i–t* experiment were evaluated as shown below. The remaining solution was then removed from the reservoir, and a new solution with another concentration was injected into the cell. The similar measurements were conducted for the new solution.

2.5. Evaluation of the methanol and water flux

The weight loss of the reservoir during the *i–t* experiment, ΔM_{LT}, which was obtained by subtracting the final weight of the remaining solution in the reservoir after the experiment, W_a, from that of the initial weight, W_0, can be expressed as follows:

$$\Delta M_{LT} = W_0 - W_a = \Delta M_{PM} + \Delta M_{PW} + \Delta M_{RM} + \Delta M_{RW} + \Delta M_V$$

where ΔM_{PM} and ΔM_{PW} are the weight losses of methanol and that of water permeating from the anode to the cathode, respectively. ΔM_{RM} and ΔM_{RW} are the weight losses of the methanol and that of water consumed by the anode reaction, respectively, and, ΔM_V is the weight loss due to the evaporation of the solution and CO_2 gas exhaust through the injection tube open to the environment.

Here, ΔM_V was experimentally confirmed that it was less than 1% of ΔM_{LT} and therefore negligible. Both ΔM_{RM} and ΔM_{RW} were calculated by integrating the area of the *i–t* curve assuming the complete oxidation of methanol:

$$CH_3OH + H_2O \rightarrow 6H^+ + CO_2 + 6e \quad (1)$$

as follows:

$$\Delta M_{RM} = \frac{32A\int_0^t i_{(t)}\,dt}{6F} \quad (2)$$

$$\Delta M_{RW} = \frac{18A\int_0^t i_{(t)}\,dt}{6F} \quad (3)$$

where A is the apparent electrode area, t is the time during the *i–t* experiment and F is the Faraday's constant. On the other hand, the weight loss of methanol from the reservoir, ΔM_{LM}, and that of water, ΔM_{LW}, was calculated as follows:

$$\Delta M_{LM} = 32(C_0V_0 - C_aV_a) \quad (4)$$

$$\Delta M_{LW} = \Delta M_{LT} - \Delta M_{LM} \quad (5)$$

where C_0 and V_0 are the concentration and volume of the methanol solution in the reservoir at the start of the experiment, respectively, and C_a and V_a are those after the experiment, respectively.

Hence, the methanol flux, J_M and water flux, J_W, that permeated through the MEA from the anode to the cathode, were calculated as

$$J_M = \frac{\Delta M_{LM} - \Delta M_{RM}}{At} \quad (6)$$

$$J_W = \frac{\Delta M_{LW} - \Delta M_{RW}}{At} \quad (7)$$

The Faraday efficiency, η_F, could be calculated as

$$\eta_F = \frac{\Delta M_{RM}}{\Delta M_{LM}} \quad (8)$$

3. Results and discussion

3.1. Current–voltage characteristics of the passive DMFC operated at different methanol concentrations with or without the porous plate

Fig. 2a and b shows the changes in the cell voltage, V, and power density, P, as a function of the current density, i, respectively, of the passive DMFC without the porous plate, i.e., a conventional MEA denoted hereafter as MEA_C, operated with various methanol concentrations from 1.0 to 5.0 M. As shown in Fig. 2a, the cell voltage at the high current densities over 50 mA cm^{-2} showed a maximum at 2 M and decreased with a further increase in the methanol concentration mainly due to the

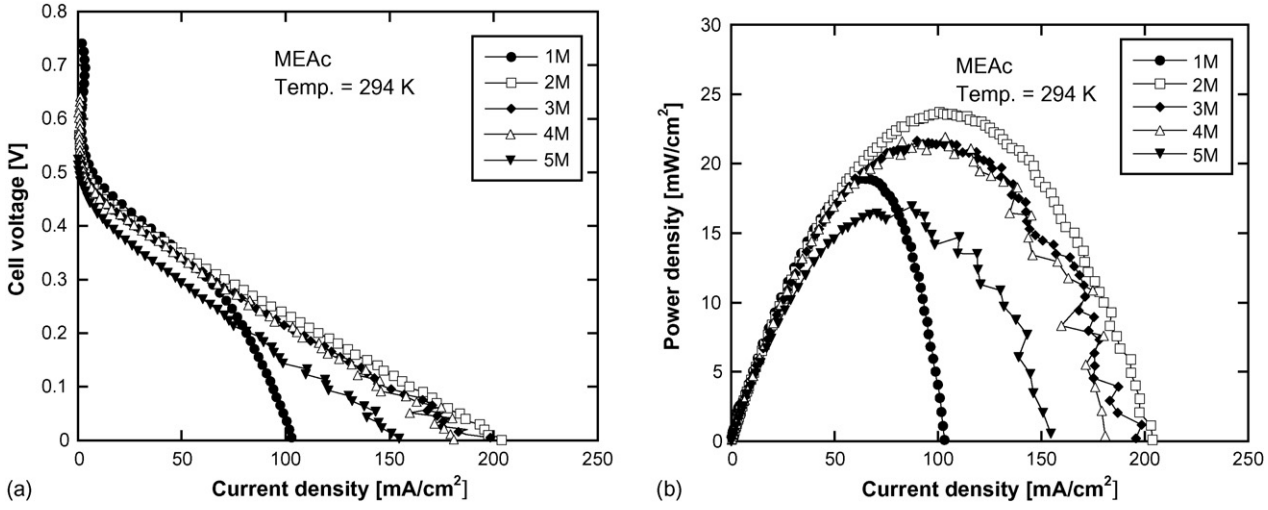

Fig. 2. Effect of methanol concentration on the performance of the passive DMFC without the porous plate, MEA_C: (a) polarization curve; (b) power density curve.

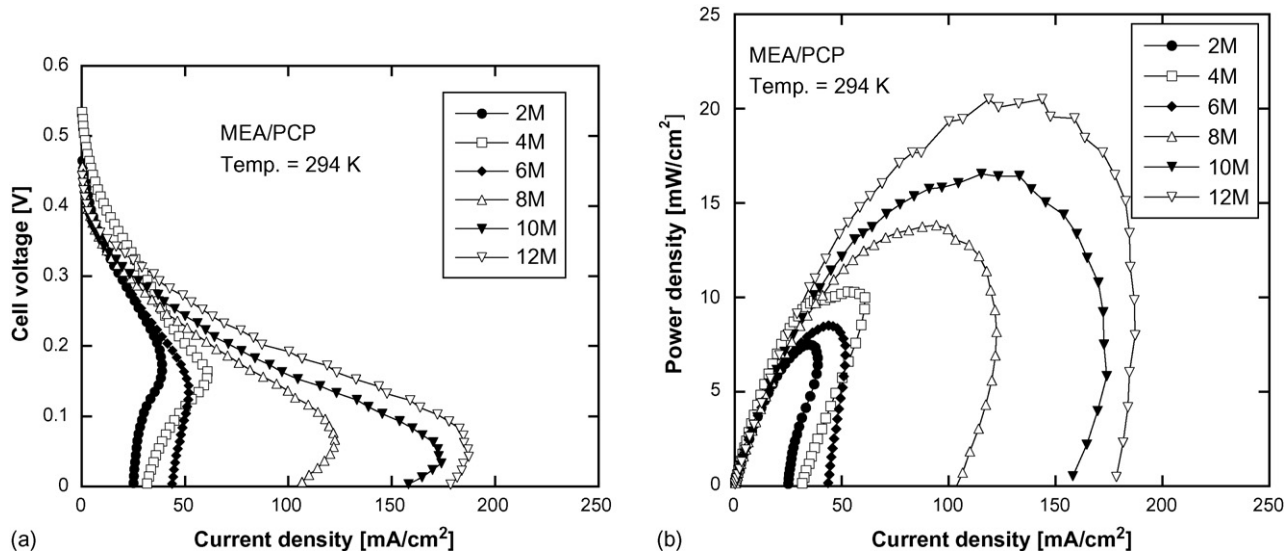

Fig. 3. The performance of the passive DMFC with the porous plate, MEA/PCP, within the low methanol concentration range from 2 to 12 M: (a) polarization curve; (b) power density curve.

methanol crossover. The maximum power density was about 24 mW cm^{-2} as shown in Fig. 2b. The current densities at low cell voltages and high methanol concentrations fluctuated and were unstable as shown in the figures. This was not due to an experimental error, and suggested that the flooding occurred at the cathode that affected the performance.

Fig. 3a and b shows the *i–V* and *i–t* performances, respectively, for the passive DMFC with PCP, denoted hereafter as MEA/PCP, operated at methanol concentrations from 2 to 12 M. At the high current densities over 50 mA cm^{-2}, the performances increased with increasing methanol concentration. At the low cell voltages, the current did not increase with the decreasing of the cell voltage at each methanol concentration, clearly showing that a limiting current occurred due to the shortage of methanol supply at the anode side. The limiting current was caused by the restriction of the methanol transfer rate from the reservoir to the anode by the porous plate [30,31] even at a high methanol concentration of 12 M in this experiment.

Fig. 4a and b shows the performances of the MEA/PCP operated at methanol concentrations over 14 M. As shown in Fig. 4a, the limiting current was not observed in the *i–V* curves as a result of increasing the concentration. The decrease in the cell voltage at almost every current density with the increasing methanol concentration over 16 M would be due to the effect of the methanol crossover. The power density at 16 M reached 24 mW cm^{-2} as shown in Fig. 4b. It should be noted that the DMFC with the PCP could be operated at a high methanol concentration of 16 M by maintaining its maximum power density like that of the DMFC without the PCP at 2 M. Fluctuation in the current density was also found in these figures at high methanol concentrations, suggesting that the flooding occurred at the conditions in the case of MEA/PCP.

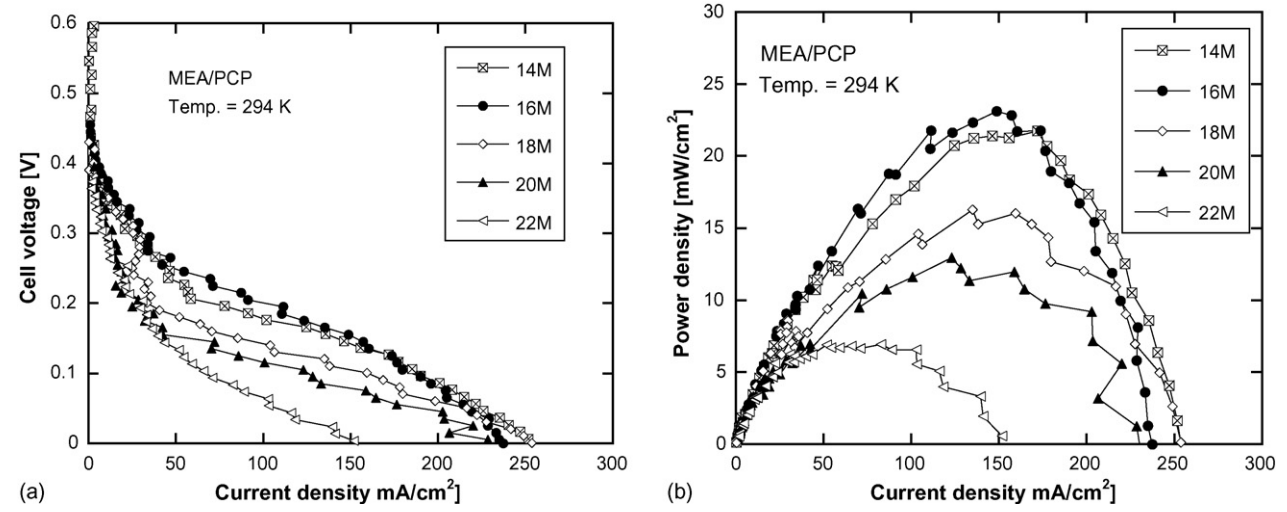

Fig. 4. The performance of the passive DMFC with the porous plate, MEA/PCP, within the high methanol concentration range from 14 M to neat methanol: (a) polarization curve; (b) power density curve.

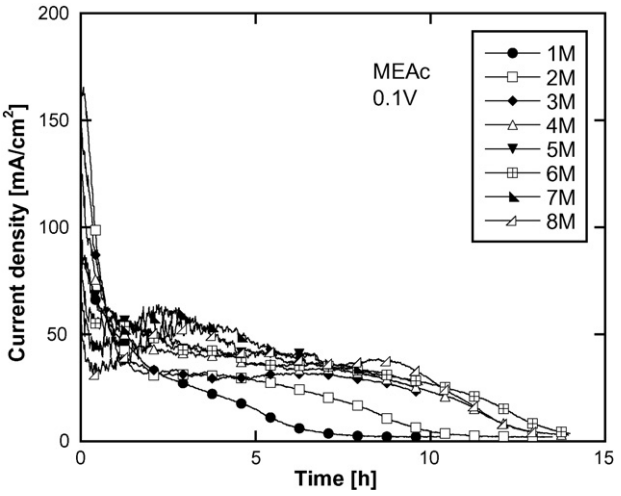

Fig. 5. Current profile during continuous operation of passive DMFC without the porous plate, MEA_C, at cell voltage of 0.1 V.

3.2. Time progress of the current at a constant cell voltage

Fig. 5 shows the current density versus time, *i–t* curves, at 0.1 V for the DMFC without the PCP, MEA_C, at different methanol concentrations from 1.0 to 8.0 M. From this figure, it was clear that the current density was initially high, then rapidly decreased to less than one-third of its initial value within 1 h. The current density further decreased with time, and, finally, reached nearly zero for all of the methanol concentrations. The time at which the current density reached nearly zero depended on the methanol concentration. The lower the concentration, the shorter the time. The rapid reduction in the initial current density would be related to the rapid depletion of the methanol at the anode due to a high MCO rate at the high methanol concentration like 8 M, or the low initial methanol at low methanol concentrations. Fluctuation in the current density was observed at high methanol concentrations over 3 M and it increased with the increasing concentration up to 8 M. It would be due to the effect of the flooding, because we visually confirmed the formation of a water film and droplets on the cathode surface under these conditions.

Fig. 6a and b shows the variations in the current density at 0.1 V for the MEA/PCP, for methanol concentrations from 2 to 12 M, and high methanol concentrations from 14 M to neat methanol, respectively. The current density somewhat initially decreased, then it was nearly constant with time within 2 h in contrast to that for the MEA_C. This was related to the employment of the PCP, which constantly regulated the methanol transfer rate from the reservoir to the anode and prevented any excess loss of methanol by the MCO. The regulation could be understood from the constant current density which almost proportionally increased with the increasing methanol concentration in the range from 2 to 16 M as shown in Fig. 6a and b. The constant current density further increased with the increasing methanol concentration until it reached a maximum, about 130 mA cm^{-2}, at 20 M, and then decreased with a further increase in the methanol concentration as shown in Fig. 6b. The decrease in the constant current density over 20 M would be due to the MCO as well as a depletion of water in the solution. An equimolar amount of methanol and water react with each other at the anode based on Eq. (1). Hence, operation at high concentrations over 17 M (=50 mol%), especially neat methanol, must requires a water supply to the anode based on a stoichiometric consideration. The optimum concentration, 20 M, that was higher than that in the case of the *i–V* curve, 16 M, as shown in Fig. 4b, was related to the relaxation time for the mass transfer in this experiment, because the current density at 16 M was the highest within the first hour from the start. The periodical fluctuation in the temperature, that appeared at the high current densities over 70 mA cm^{-2}, except for the case with the neat methanol, was related to the periodical changes in the ambient room temperature with ±1 K controlled by an air conditioner. Neither a water film nor water droplets were found at the cathode surface, during the experiment for MEA/PCP even for neat methanol, suggesting that the electrode was free from flooding.

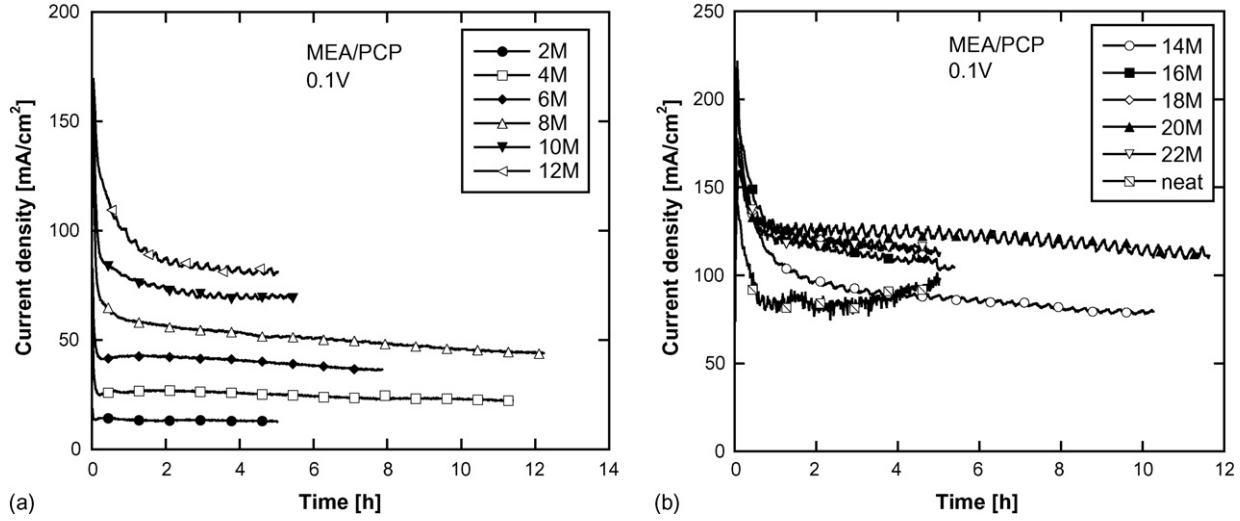

Fig. 6. Current profile during continuous operation of passive DMFC with the porous plate, MEA/PCP, at cell voltage of 0.1 V: (a) with methanol concentration from 2 to 12 M; (b) with methanol concentration from 14 M to neat methanol.

Although the current density was relatively low, it was demonstrated that the neat methanol could be used as shown in Fig. 6b. The current density was initially low then slightly increased with time. This slight increase in the performance would be caused by the water supply from the cathode to the anode due to the back diffusion of water as will be mentioned later.

3.3. Influence of methanol concentration on the cell temperature

Fig. 7 shows the changes in cell temperature during the *i–t* experiment, Fig. 5, for the MEA_C. The lines show a moving average temperature, because the cell temperature fluctuated, within ±1 K from the line, accompanied with the change of the ambient temperature controlled by an air conditioner. The cell temperature initially increased to a certain level then decreased showing a peak in the temperature profile. As the methanol concentration increased, the level of the peak increased. When the concentration was as high as 8 M, the temperature increased from 298 to 315 K and then decreased. It has already been pointed out that the cell temperature of a passive DMFC is generally related to the magnitude of the MCO [11,16] and also the increase in the temperature by the MCO reflexively accelerates the MCO [31]. The depletion in the methanol at the anode would decrease the MCO and then the temperature after the peak.

Fig. 8 shows the cell temperature for the MEA/PCP at different methanol concentrations from 4 M to neat methanol, corresponding to the *i–t* experiment shown in Fig. 6a and b, in the similar way of the representation as shown in Fig. 7. It was clearly shown in this figure that the employment of the PCP kept the cell temperature low and constant compared to that for the MEA_C, where, the temperature of the MEA/PCP at 8 M was about 297 K, but it was greater than 315 K for the MEA_C at the same concentration. The temperature for MEA/PCP relatively decreased with time after several hours due to the decrease in the MCO that resulted from the decrease in the methanol concentration with time. The cell temperature increased with increasing methanol concentration and reached about 318 K for neat methanol.

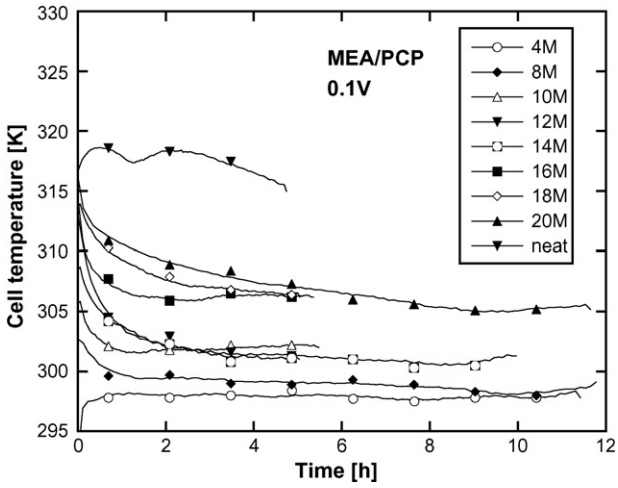

Fig. 8. Variations in operating cell temperature of passive DMFC with the porous plate, MEA/PCP, at cell voltage of 0.1 V. The plot shows an actual temperature and the line shows moving average temperature.

The initial temperatures for the MEA/PCP were higher than that for the MEA_C due to the MCO during the open circuit situation before the *i–t* measurement. Before starting the *i–t* measurement, the cell, in case of the MEA/PCP, was maintained at open circuit situation for a certain time from a few minutes to more than 1 h based on the methanol concentration in order to make the methanol concentration at the anode surface close to that of the solution in the reservoir, after the injection of the solution with a certain methanol concentration into the reservoir. During this open circuit situation, the temperature of the MEA/PCP somewhat increased.

It was very clear from Figs. 7 and 8 that the temperature profile coincided with the current profile, suggesting that the performance was sensitive to the temperature.

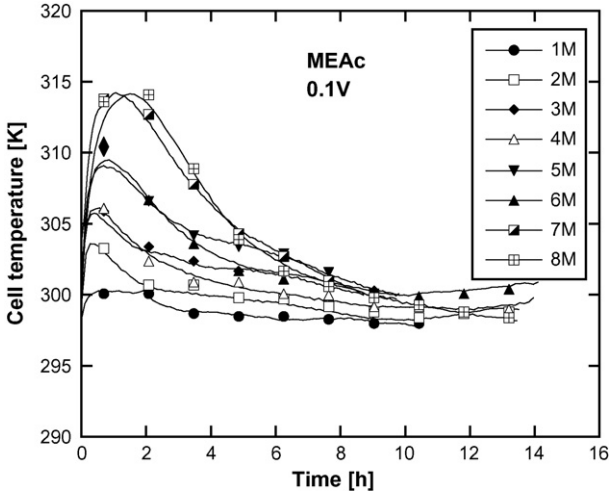

Fig. 7. Variations in operating cell temperature of passive DMFC without the porous plate, MEA_C, at cell voltage of 0.1 V. The plot shows an actual temperature and the line shows moving average temperature.

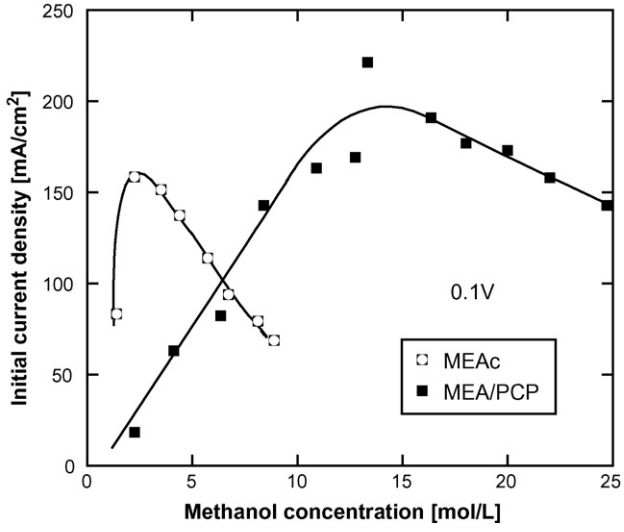

Fig. 9. Effect of methanol concentration on initial current density for MEA with and without the porous plate.

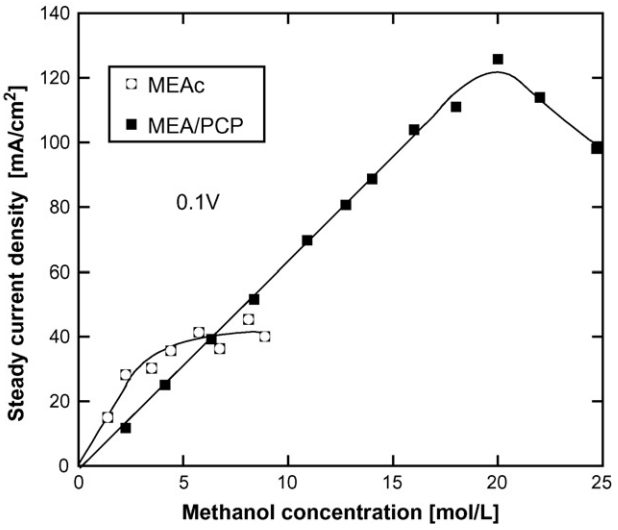

Fig. 10. Effect of methanol concentration on steady current density for MEA with and without the porous plate.

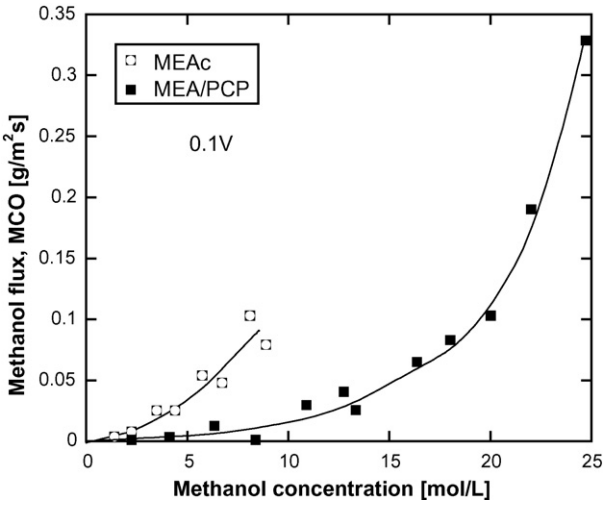

Fig. 11. Effect of methanol concentration on methanol crossover for MEA with and without the porous plate.

Fig. 9 shows the effect of the methanol concentration on the initial current density, the peak current density appeared within 5 min from the start, for the MEA with and without the porous plate. The peak current density reached the maximum, 160 mA cm^{-2}, at 2 M for the MEA_C, but decreased with the increasing methanol concentration. On the other hand, in the case of the MEA/PCP, the initial current density reached about 190 mA cm^{-2} at the methanol concentrations ranging from 12 to 20 M. A similar peak current density, but at different methanol concentrations for the MEA_C and MEA/PCP suggested that the mass transfer of methanol was restricted at the MEA/PCP, but the electrode activity was reproduced with the high methanol concentrations at the MEA/PCP.

Fig. 10 shows the effect of the methanol concentration on the steady current density, which was defined as the current density at 300 min from the start, for the MEA_C and MEA/PCP. In the case of the MEA_C, the steady current density increased with the increasing methanol concentration from 1 to 4 M and reached about 40 mA cm^{-2}; this value slightly increased with the increasing concentration up to 8 M. On the other hand, for the MEA/PCP, the steady current density increased with the increasing methanol concentration and reached about 130 mA cm^{-2} at 20 M, which was three times higher than that for the MEA_C and was similar to the maximum initial current density for the MEA_C. The proportional dependency of the current density on the concentration up to 20 M meant, again, that the methanol supply to the anode was the rate limiting step.

This figure clearly showed the significant effect of employing the PCP, i.e., a very high methanol concentration like 20 M could be used, and the current density was three times higher than that for the MEA_C.

3.4. Permeation of methanol and water through membrane

Fig. 11 shows the effect of the methanol concentration on the MCO as the methanol flux through the membrane, J_M, defined by Eq. (6), for MEA_C and MEA/PCP. As shown in the figure, the MCO for both MEA_C and MEA/PCP increased with the increasing methanol concentration, but differently. It would be due to the increase in the driving force of the methanol transfer, i.e., the difference in the concentration of methanol between the anode surface and the cathode surface. It was very clear in the figure that the MCO for MEA/PCP at any methanol concentration was very small, about 1/10, in comparison to that for the MEA_C. And then, the MCO for MEA_C at 7 M was nearly equivalent to that for the MEA/PCP at 20 M.

On the other hand, Fig. 12 shows the effect of the methanol concentration on the water flux through the membrane, J_W, defined by Eq. (7), for MEA_C and MEA/PCP. As shown in the figure, the water flux for MEA_C was about 0.1 g m^{-2} s^{-1}) and this value was not affected by the methanol concentration. Whereas, in the case of MEA/PCP, the water flux decreased with the increasing concentration, and, noteworthy, it became negative from 6 M and further decreased as the methanol

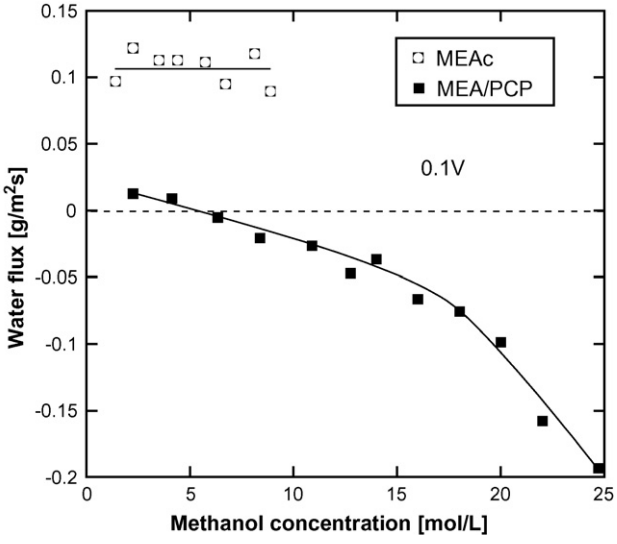

Fig. 12. Effect of methanol concentration on water flux for MEA with and without the porous plate.

concentration increased. The negative flux meant the back diffusion of water from the cathode to the anode. The magnitude of the back diffusion of water increased with the increasing concentration. This must be a result of the balance of water that was consumed at the anode and that supplied from the reservoir and from the cathode through the membrane. Water can be supplied not only from the reservoir, but also from the cathode where water is produced by the oxygen reduction reaction and by the oxidation of the permeated methanol. The back diffusion of water from the cathode was desirable for the DMFC to prevent the cathode from flooding. Actually, neither a water film nor water droplets were observed at all on the cathode surface during the *i–t* experiments for the MEA/PCP, whereas, flooding was very clear at the cathode in case of the MEA_C. This would be one of the main reasons for the MEA/PCP to have superior *i–t* performances compared to that for the MEA_C.

As shown in Figs. 11 and 12, it was clear that not only the methanol flux, but also the water flux were significantly reduced by employing the PCP. In our previous paper, we found that the PCP controlled the methanol flux and water flux through the membrane under open circuit conditions by the diffusion resistance of the PCP [31]. Different from the cases of the open circuit conditions, we need to consider effect of CO_2 gas that was produced at the anode. The CO_2 gas would be accumulated in the space between the anode and the porous plate and also in some of the pores of the PCP preparing a layer of CO_2 gas. Once the gas layer was formed, it was maintained during the experiment. This CO_2 gas layer must add an additional resistance to the mass transport, because the CO_2 has to be transported from the anode to the outlet through the PCP in a counter flow to that of the methanol and the water, in this experiment. Also, the methanol and the water have to be transported as gaseous materials in the gas layer with the CO_2. Hence, these effects significantly reduced the rate of the mass transport of methanol and water from the reservoir to the anode, which resulted in a very strong reduction of the MCO and negative flux of water as shown in the figure. We postulate that the PCP and the CO_2 gas layer acted as a barrier for the methanol and water transport, where the PCP was necessary to prepare and stably maintain the CO_2 layer over the anode surface.

To check the effect of the CO_2 barrier on the cell performance, we changed the distance between the anode and the PCP using two current corrector plates at the anode. Fig. 13 shows the effect of the distance between the PCP and the anode surface on the steady current density at the cell voltage of 0.1 V. In this experiment, a different MEA with a somewhat different catalyst loading from that used in the above figures was used. The result with a 2 mm distance was not the same as that shown in Fig. 10. From this figure, it was clear that, as the distance increased from 2 to 4 mm, the steady current density decreased from 140 mA cm^{-2} at 16 M to 100 mA cm^{-2} at 20 M. This could be explained by the fact that as the distance between the PCP and the anode surface increased, the resistance to the mass transfer increased, so the performance at a certain concentration decreased and the optimum concentration increased from 16 to 20 M, to compensate for the methanol supply from the reservoir.

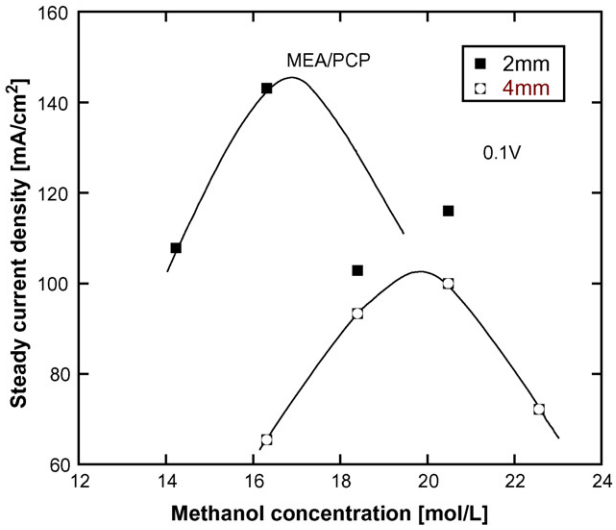

Fig. 13. Effect of the distance between the anode and the porous plate on the performance of the passive DMFC.

Fig. 14 shows the comparison of the Faraday efficiency between the MEA_C and MEA/PCP corresponding to the results shown in Figs. 5–12. It should be noted that, in case of the MEA/PCP, the Faraday efficiency was significantly higher than that in the case of MEA_C over the entire range of measured methanol concentrations. In the case of MEA_C, the Faraday efficiency decreased from 75% at 1 M to about 30% at 5 M. Contrary to this, it only decreased from 80% at 2 M to 60% at 14 M in the case of MEA/PCP. The Faraday efficiency for the MEA_C at 5 M was nearly the same as that at 22 M for MEA/PCP. This was a direct result of controlling the MCO by employing the PCP showing that the methanol was efficiently converted to a power output, and also that a very high methanol concentration could be efficiently used. The efficient utilization of the methanol in the MEA/PCP was also explained in Fig. 15 that shows the relationships between W_a/W_0 and C_a/C_0 for the *i–t*

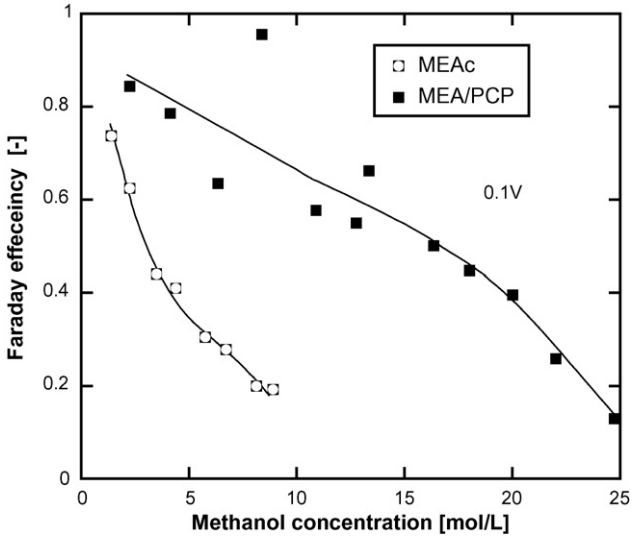

Fig. 14. Effect of methanol concentration on faradic efficiency for MEA with and without the porous plate.

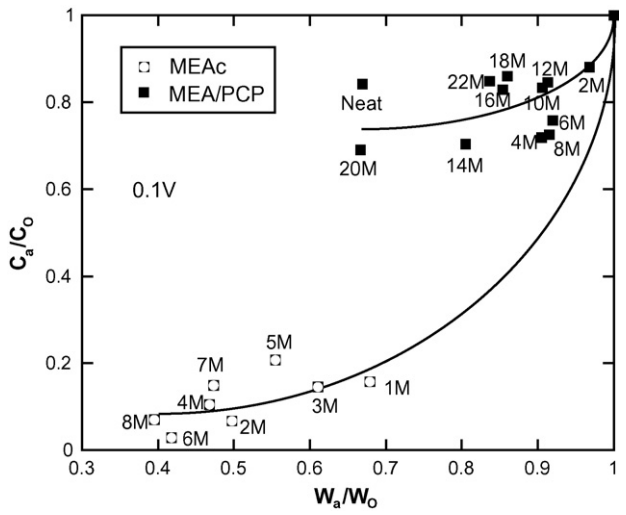

Fig. 15. Relationship between the decrease in the weight and that of the methanol concentration for the methanol solution remaining in the reservoir during the experiments of the MEA with and without the porous plate.

experiments corresponding to Fig. 14. We can see in this figure that how the concentration and the weight of the input methanol solution changed during the *i–t* experiments for both the MEA_C and MEA/PCP.

As shown above, the employment of the porous plate made the efficient utilization of the high methanol concentrations possible by controlling the mass transport from the reservoir to the anode. The employment of PCP is quite effective for achieving an efficient DMFC and an important technique to increase its power density. The back diffusion of water from the cathode to anode was confirmed at the high methanol concentrations. This back diffusion of water through the Nafion membrane with a high water permeability would be essential for achieving a high performance with this type of mechanism using the porous plate. Although the power output, 24 mW cm^{-2}, obtained in this study may not be enough for an actual DMFC, we can expect a higher performance by optimizing the catalyst layer and also the other electrode structure including the distance between the anode and the porous plate as well as the pore structure of the porous plate. The *i–t* performance with different cell voltages and with different porous plates for the MEA/PCP is currently under investigation by the authors. It will be reported in the near future.

4. Conclusions

Performance of the passive DMFC with and without the PCP was investigated under closed circuit conditions with different methanol concentrations ranging from 1 M to neat methanol, and the following conclusions were drawn:

(1) Mass transfers both of the methanol and water from the reservoir to the anode were significantly restricted by the employment of the PCP on the anode side. It was considered that the CO_2 gas layer formed between the anode and PCP restricted the mass transfer, and the PCP stably maintained the CO_2 layer over the anode.

(2) As a result of the mass transfer restrictions by employing the PCP, high methanol concentrations, even neat methanol, could be efficiently used. This resulted in a high power density for the DMFC.

(3) The back diffusion of water from the cathode to the anode was confirmed at relatively high methanol concentrations for the DMFC with PCP. This was required in order to prevent the cathode from flooding and increased the cell performance.

Acknowledgments

The authors acknowledge the New Energy and Industrial Technology Development Organization (NEDO) for their financial support of this study and Mitsubishi Pencil Co. Ltd., for the preparation and gift of the porous carbon plate.

References

[1] H. Chang, J.R. Kim, J.H. Cho, H.K. Kim, K.H. Choi, Solid State Ionics 148 (2002) 601–606.
[2] Blum, T. Duvdevani, M. Philosoph, N. Rudoy, E. Peled, J. Power Sources 117 (2003) 22–25.
[3] D. Kim, E.A. Cho, S.A. Hong, I.H. Oh, H.Y. Ha, J. Power Sources 30 (2004) 172–177.
[4] Z. Guo, Y. Cao, J. Power Sources 132 (2004) 86–91.
[5] T. Shimizu, T. Momma, M. Mohamedi, T. Osaka, S. Sarangapani, J. Power Sources 137 (2004) 277–283.
[6] H. Qiao, M. Kunimatsu, T. Okada, J. Power Sources 139 (2005) 30.
[7] Q. Ye, T.S. Zhao, J. Power Sources 147 (2005) 196–202.
[8] B. Kho, I. Oh, S. Hong, H.Y. Ha, Electrochim. Acta 50 (2004) 781.
[9] A.S. Arico, S. Srinivasan, V. Antonucci, Fuel Cells 1 (2001) 133–161.
[10] T. Schultz, S. Zhou, K. Sundmacher, Chem. Eng. Technol. 24 (2001) 1223–1233.
[11] J.G. Liu, T.S. Zhao, R. Chen, C.W. Wong, Electrochem. Commun. 7 (2005) 288.
[12] J.G. Liu, T.S. Zhao, Z.X. Liang, R. Chen, J. Power Sources 153 (2006) 61–67.
[13] S. Surampudi, S.R. Narayanan, E. Vamos, H. Frank, G. Halpert, A. LaConti, J. Kosek, G.K. Surya Prakash, G.A. Olah, J. Power Sources 47 (1994) 377–385.
[14] M.K. Ravikumar, A.K. Shukla, J. Electrochem. Soc. 143 (1996) 2601–2606.
[15] S.R. Yoon, G.H. Hwang, W.I. Cho, I.-H. Oh, S.-A. Hong, H.Y. Ha, J. Power Sources 106 (2002) 215–223.
[16] R. Chen, T.S. Zhao, J. Power Sources 152 (2005) 122–130.
[17] B. Bae, B.K. Kho, T. Lim, I. Oh, S. Hong, H.Y. Ha, J. Power Sources 158 (2006) 1256–1261.
[18] J.T. Wang, S. Wasmus, R.F. Savinell, J. Electrochem. Soc. 143 (1996) 1233–1239.
[19] E. Peled, T. Duvdevani, A. Aharon, A. Melman, Electrochem. Solid State Lett. 3 (2000) 525–528.
[20] M.V. Fedkin, X. Zhou, M.A. Hofmann, E. Chalkova, J.A. Weston, H.R. Allcock, S.N. Lvov, Mater. Lett. 52 (2002) 192–196.
[21] T. Yamaguchi, M. Ibe, B.N. Nair, S. Nakao, J. Electrochem. Soc. 149 (2002) A1448–A1453.
[22] M.L. Ponce, L. Prado, B. Ruffmann, K. Richau, R. Mohr, S.P. Nunes, J. Membr. Sci. 217 (2003) 5–15.
[23] A.S. Arico, P. Creti, P.L. Antonucci, V. Antonucci, Electrochem. Solid State Lett. 1 (1998) 66–68.
[24] C. Yang, S. Srinivasan, A.S. Arico, P. Creti, V. Baglio, V. Antonucci, Electrochem. Solid State Lett. 4 (2001) A31–A34.

[25] N. Jia, M.C. Lefevre, J. Halfyard, S. Qi, P.G. Pickup, Electrochem. Solid State Lett. 3 (2000) 529–531.
[26] I.J. Hobson, H. Ozu, M. Yamaguchi, M. Muramatsu, S. Hayase, J. Mater. Chem. 12 (2002) 1650–1656.
[27] W.C. Choi, J.D. Kim, S.I. Woo, J. Power Sources 96 (2001) 411–414.
[28] S.R. Yoon, G.H. Hwang, W.I. Cho, I.-H. Oh, S.-A. Hong, H.Y. Ha, J. Power Sources 106 (2002) 215–223.
[29] Y.K. Xiu, K. Kamata, T. Ono, K. Kobayashi, T. Nakazato, N. Nakagawa, Electrochemistry 73 (2005) 67–70.
[30] N. Nakagawa, K. Kamata, A. Nakazawa, M. Ali Abdelkareem, K. Sekimoto, Electrochemistry 74 (2006) 221–225.
[31] N. Nakagawa, M. Ali Abdelkareem, K. Sekimoto, J. Power Sources, in press.
[32] G.Q. Lu, C.Y. Wang, T.J. Yen, X. Zhang, Electrochim. Acta 49 (2004) 821.
[33] C.Y. Chen, P. Yang, J. Power Sources 123 (2003) 37–41.
[34] R. Chen, T.S. Zaho, J.G. Liu, J. Power Sources 157 (2006) 351–357.
[35] J. Liu, G. Sun, F. Zhao, G. Wang, G. Zhao, L. Chen, B. Yi, Q. Xin, J. Power Sources 133 (2004) 175–180.
[36] S. Yao, X. Tang, C. Hsieh, Y. Alyousef, M. Vladimer, G. Fedder, C. Amon, Energy 31 (2006) 636–649.